Journal of Alloys and Compounds 501 (2010) 345–351

Contents lists available at ScienceDirect

Journal of Alloys and Compounds

journal homepage: www.elsevier.com/locate/jallcom

Spark plasma sintering of α-Si_3N_4 ceramics with Al_2O_3 and Y_2O_3 as additives and its morphology transformation

L. Ceja-Cárdenas [a,*], J. Lemus-Ruíz [a], D. Jaramillo-Vigueras [b], S.D. de la Torre [b]

[a] Instituto de Investigaciones Metalúrgicas, UMSNH. Edif. "U", CU., C.P. 58000 Morelia, Mich., Mexico
[b] Instituto Politécnico Nacional, CIITEC. Cerrada Cecati s/n Col. Sta. Catarina, C.P. 02250 Azc., D.F., Mexico

ARTICLE INFO

Article history:
Received 22 January 2010
Accepted 7 April 2010
Available online 24 April 2010

Keywords:
Spark plasma sintering
Alpha α- and beta β-Si_3N_4
Phase transformation
Al_2O_3 and Y_2O_3
Rod crystals morphology

ABSTRACT

The spark plasma sintering SPS technique has been used to densify pure α-Si_3N_4 commercial powder, having Y_2O_3 and Al_2O_3 additions; from 0, 2.5 and 5.0 wt% to 0, 1.5 and 3 wt%, respectively. Such powder admixtures were previously spray-dried at 160 °C in such a way that powder was thoroughly homogenized. Set sintering treatment included: 0–20 min holding time and 38 MPa axial load, sintering temperature of 1500 °C and heating rate of 300 °C/min. The maximum relative density developed on studied specimens ranged from 99.4 to 99.8% and could only be attained once the β-phase nucleated from the α-silicon nitride matrix. Obtained Si_3N_4 composites combine both α- and β-phases. The later phase becomes evident trough the rod-like geometry, which forms throughout the presence of a liquid face. The largest hardness value developed (1588 $Hv_{(20\,kgf)}$) on studied ceramics (3M-series – 3 min) matched close to the corresponding counterpart found in literature (1600 Hv), the former developed in much shorter sintering times. Using X-ray diffraction XRD and scanning electron microscope SEM analyses, the two major phases of Si_3N_4 were identified in the resultant microstructures. The morphology evolution of Si_3N_4 particles as occurred upon SPS-sintering is analyzed.

1. Introduction

Silicon nitride (Si_3N_4) is one of the most attractive advanced ceramic materials for specific applications since the resulting microstructure of these ceramics after sintering is similar to that of whisker-reinforced composites, exhibiting rod-like β-Si_3N_4 grains which act as strengthening/interlocking elements [1]. Moreover, this ceramics are used on a variety of structural applications, due to its excellent mechanical properties either at ambient or elevated temperatures. Design engineering of gas turbines involves these materials due not only to high temperature performance but also thermal shock resistance, which may eliminate the need for a cooling system. Sufficient fracture toughness, high hardness and excellent wear resistance are important features sought in advanced ceramics for applications in cutting tools and automotive components such as diesel engine cam rollers and ball bearings. It is also important to develop high performance Si_3N_4 ceramics against corrosion attack at high temperatures. All these factors have attracted considerable attention from the academic and industrial communities [2–4].

Silicon nitride ceramics have been fabricated by a number of techniques, including reaction bonding, gas pressure sintering, hot-pressing, pressure-less sintering and hot isostatic pressing [5]. However, Si_3N_4 cannot be easily densified by solid state sintering and the task of obtaining fully dense microstructure bulk samples has received considerable attention in various fields of the materials engineering [6,7]. Spark Plasma Sintering (SPS) is a non-conventional powder consolidation method, which has shown to be effective in sintering a number of novel materials difficult or impossible to sinter by ordinary techniques. One of the major differences found between other sintering process and SPS is the heating rate. Powder densification takes place in SPS through the usage of a pulsed direct current which passes thought the electrically conducting die and sample holder, so that the Joule-heat effect takes place almost instantaneously promoting fast sintering of powders [8].

On sintering Si_3N_4 powder it is common practice to use flux additives in order to assist sintering via a liquid phase [9–12]. If the liquid phase is in excess it might then remain as amorphous grain boundaries upon cooling. The nature of such grain boundaries in Si_3N_4 ceramics greatly determines the final properties of bulk materials. It is thus important to make not only the appropriate selection of additives but also the amount (mixture) to be used. Using the SPS-technique and MgO–$AlPO_4$ as sintering additives Chen et al. [13] reported sintering of α-Si_3N_4 ceramics. They found

* Corresponding author.
E-mail addresses: leocc4@yahoo.com.mx, sediazt@ipn.mx (L. Ceja-Cárdenas).

0925-8388/$ – see front matter © 2010 Elsevier B.V. All rights reserved.
doi:10.1016/j.jallcom.2010.04.102

Table 1
Code and chemical composition of SPS-treated specimens (wt%).

Mixture	α-Si_3N_4	Y_2O_3	Al_2O_3
M1	100	0	0
M2	96	2.5	1.5
M3	92	5	3

better densification of their Si_3N_4 ceramics provided sintering additives changed from 6 to 20 wt% and temperatures from 1300 to 1550 °C. They argued that there is a reaction between MgO and SiO_2 whose product adhere and react with $AlPO_4$. They concluded that bending strength of their ceramics is in close correlation with relative density and the content of $AlPO_4$ additives. Gui-hua et al. [14] also used SPS-technique to sinter α-Si_3N_4 ceramics with $MgSiN_2$ and attributed high mechanical properties (fracture toughness of 7.7 MPa $m^{1/2}$) to the fact of controlling the α/β-phase composition and microstructure of their ceramics. Some other research conducted on SPS-treated Si_3N_4 ceramics reported on improving mechanical properties by combining Si_3N_4/SiC nanocomposites with reduced additive amounts [15], as well as Si_3N_4/BN [16]. The former concluded that the additive amounts have a drastic effect on the microstructure and phase composition of studied ceramics. They claimed that when the sintering temperature is too high, a decrease in the additive amount can bring about severe decomposition of silicon nitride phase, which in turn leads to grain growth of the silicon carbide phase.

In general, on sintering α-Si_3N_4 free powder, additives such as alumina, magnesia, yttria, nitrides and/or different rare earth oxides are used for easier and higher densification, which can be added alone or in combination. To better take advantage of final properties of Si_3N_4 ceramics some authors design specific microstructures such that the α → β transformation of Si_3N_4 is controlled by rapid sintering either to avoid grain growth, to develop bimodal particles and/or manipulating phase transformation (seeding), as well as doping matrix with additives. In the case of Si_3N_4 ceramics it is now accepted that grain growth of elongated grains is predominantly diffusion-controlled [16]. Although, the sintering process of Si_3N_4 has been widely investigated, some experimental parameters, such as the amount and type of additives still need to be investigated when superfast sintering is used. The sintering time has significant influence on the density and phase transformation of this ceramics [17]. This work aims to sinter α-Si_3N_4 powder with different amount of additives, using the Spark Plasma Sintering technique and gives an explanation of the particles change morphology followed when the α- to β-Si_3N_4 transformation takes place.

2. Experimental procedure

Commercial α-Si_3N_4 powder (Toshiba Ceramics Co., Ltd., USA) of 1.1 μm mean size, 99.9% purity was used to conduct this investigation. Oxide additives such as Y_2O_3 (99.9%) Molycorp Minerals, USA and Al_2O_3 (99.99%) Taimei Chemicals Co., Ltd., Tokio, Japan were used as sintering aids. To analyze the amount effect of additives on the sintering process, three compositions were prepared (see Table 1). Selected compositions were mixed using Spray Drying technique (Mini-Spray Dryer ADL 31). A powder suspension was first prepared (liquid to powder ratio of 1:15 by weight). The product was then magnetically agitated for 30 min at 720 rpm before being spray-dried in the equipment, setting a flow velocity of 0.4 l/h while temperature inside the drying chamber set at 160 °C. The specimens were designed as specified in Table 1 and green-compacted using a graphite dies set with an inner diameter of ϕ10 mm. Sintering runs were conducted using a commercial spark plasma sintering device (Sumitomo Dr. Sinter, SPS-1050) with on/off current pulses of 12/2, 3500Amp and 4 V. Established sintering treatment included: 0–20 min holding time and 38 MPa axial load, sintering temperature of 1500 °C and heating rate of 300 °C/min. Specimens were hold at that temperature for 0, 3 and 20 min before being cooled down inside the furnace. The sintering temperature was measured attaching a digital pyrometer, directly aligned onto the surface of the graphite die. Both constant load pressure and vacuum atmosphere of 0.5 Pa were kept from the beginning to the end of each sintering cycle.

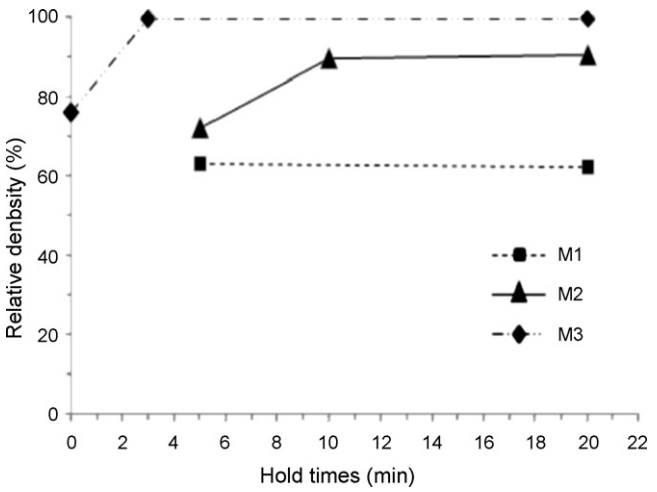

Fig. 1. Relative density of 1500 °C sintered Si_3N_4 ceramics plotted as a function of soaking time (Table 1).

The bulk density of resulting specimens was measured by the Archimedes's immersion principle using distilled water. Microstructure phase identification analysis was carried out by using X-ray diffraction (XRD) with Cu Kα radiation, at an accelerating voltage of 30 kV and current density of 20 mA. X-ray scanned from 10 to 90 ($2\theta^{\circ}$), at an angular velocity of 2.0° min^{-1}. The morphology and physical condition of fractured surfaces of studied materials were observed using JEOL JSM-6400 scanning electron microscope (SEM). Specimens were chemically etched with hydrofluoric acid at room temperature for 30 min to reveal microstructural details. Vickers hardness was measured along twelve indentation points on perfect-polished surfaces for each sample, using Vickers Hardness tester equipment (HWDV-7). Hardness load and loading time were set to 20 kg^f and 5 s, respectively.

3. Results and discussion

Fig. 1 shows the relative density of Si_3N_4–Y_2O_3–Al_2O_3 ceramics treated by SPS at 1500 °C, plotted versus the holding time upon sintering, using the amount of additives described in Table 1. In all studied cases, the relative density further developed by increasing the amount of additives. It is confirmed that if no additives were used into the α-Si_3N_4 powder matrix, case M1, there will be neither more densification nor phase transformation (Fig. 4). To be noted is the fact that allowing holding time along the sintering course, and once the silicon nitride matrix is at 1500 °C denser bodies are obtained, provided a given amount of additives are supplied into the matrix. Thus, 3 and 10 min soaking time is needed for M3 and M2 specimens to densify, respectively. From literature it is known that a glassy phase usually forms in silicon nitride ceramics when they are sintered at high temperatures [9–11]. Such phase is made out of a silica (SiO_2) surface layer, which is derived in turn from nitrogen (Si–N) volatilization and is a result of the reaction occurring between the sintering aids (Y_2O_3–Al_2O_3). The silica surface layer wets silicon nitride grains promoting sintering, so that liquid phase founds its equilibrium place at the grain boundaries.

The maximum relative density attained in all studied cases was that disclosed from M3 specimens with 99.4 and 99.8% for 3 and 20 min holding times, respectively. Analyzing Fig. 1 it is evident that the more amount of additives the larger densification level developed on those specimens. Evidently, the usage of more amounts of additives might increase the sintering cost of Si_3N_4-based products at industrial scale, apart from spoiling mechanical properties due to an excess of glassy phase. Setting few amount of additives and expanding the soaking time, case M2, however, does not solve the economic problem since more energy is then required.

Fig. 2 shows three samples ϕ10 mm in diameter of the M2-series revealing that no further sintering shrinkage takes place on the specimens after 10 min at 1500 °C. A 90% of the relative density

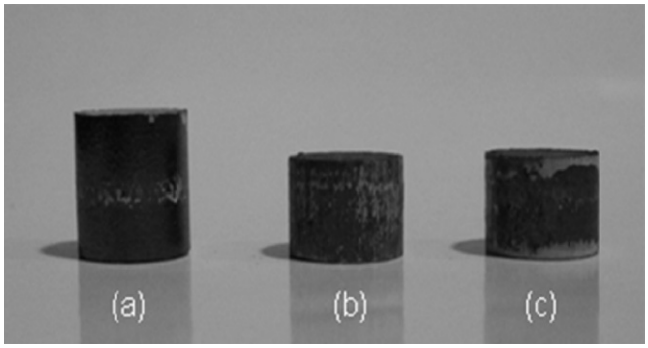

Fig. 2. M2-specimens sintered at 1500 °C for (a) 5, (b) 10 and (c) 20 min. All specimens were originally prepared using 1.5 g of powder. No further shrinkage is evident after 10 min soaking time.

is only obtained when the yttria and alumina content add 4 wt%. It seems that giving the Si_3N_4 powder nature used in this work, such as particle size, morphology and purity, as well as the powder conditioning treatment set, more amount of additives is required. From this experiments it cannot be explained the isolated effect or contribution of yttria or alumina for promoting densification on Si_3N_4.

Fig. 3 shows powder morphology and fractured surface of Si_3N_4 samples having no additives. Fig. 3(a) corresponds to the as-received pure α-Si_3N_4 powder. Fig. 3(b) shows same powder after being sintered at 1500 °C for 20 min, M1. A comparison made on these two SEM pictures reveals no rheological differences between particles. XRD analysis confirmed the exclusive presence of alpha phase (see Figs. 4 and 5). Powder remained practically un-reacted but slightly agglomerated (around 60% relative density) after sintering.

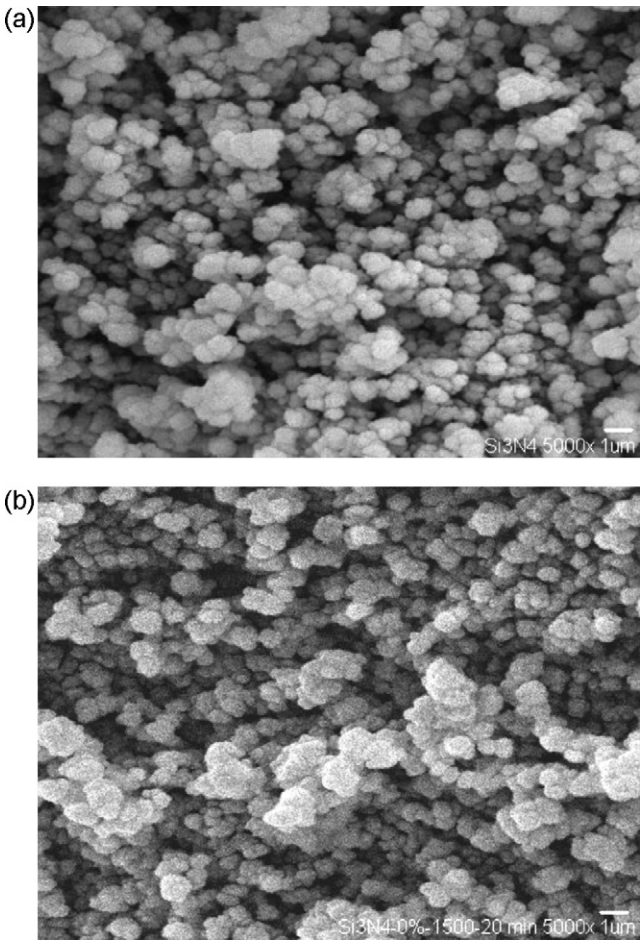

Fig. 3. Powder morphology and fractured surface of Si_3N_4 samples having no additives. (a) As-received pure α-Si_3N_4 powder, and (b) same powder after being sintered at 1500 °C for 20 min, M1. Powder remained practically un-reacted but slightly agglomerated (60% relative density).

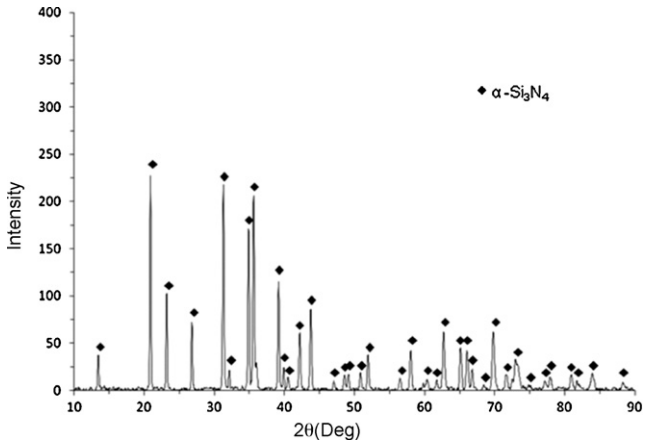

Fig. 4. XRD-pattern of M1-specimen sintered at 1500 °C for 20 min. The relative density of this specimen is about 60%.

Figs. 4 and 5 show X-ray diffraction patterns of the M1- and M2-series specimens, respectively. Fig. 4 reveals that no phase transformation has occurred on the precursor powder in spite of the fact that sintering time lasted for 20 min. The last is particularly true for the case of a silicon nitride α-matrix having no additives. Pure silicon nitride is a basically covalent compound and its bulk diffusion is too low to be fully consolidated. Therefore, oxides or nitrides sintering additives are necessary to fabricate high-density silicon nitride ceramics by liquid phase sintering [12].

On the other hand, the α- to β-phase transformation became evident after allowing 10 min soaking time for those analyzed samples upon SPS-sintering, Fig. 5. The later samples have 4 wt% total additives (Y_2O_3–Al_2O_3) and were sintered at 1500 °C at different holding times; namely 5, 10 and 20 min. Although the 5 min set specimen could not achieve phase transformation, the attained densification level was better than that of the specimen sintered at similar holding time M1 (Fig. 1). The later fact is due to formation of the liquid phase that reduces the activation energy and promotes

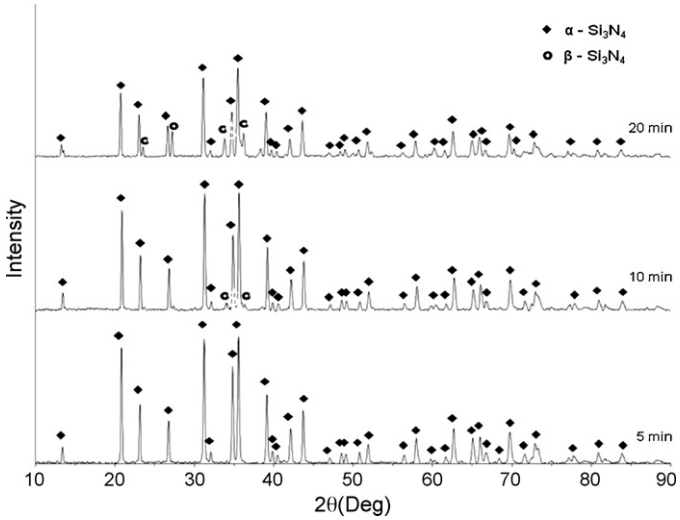

Fig. 5. XRD-patterns of M2-specimens sintered at 1500 °C with holding sintering times of 5, 10 and 20 min.

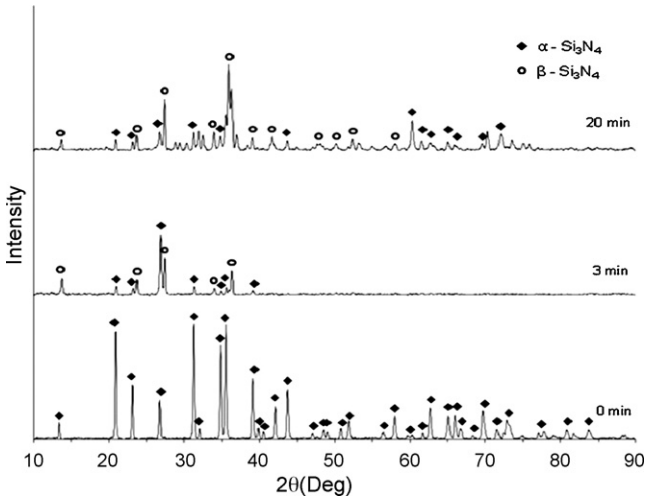

Fig. 6. XRD-patterns of M3-specimens sintered at 1500 °C with holding sintering times of 0, 3 and 20 min.

densification [4]. The presence of the β-phase in Si_3N_4 becomes evident, as detected by XRD at holding times above 10 min. Although on further soaking times (20 min) the α- to β-phase transformation keeps on going, considerable amount of alpha phase still remains in the ceramic microstructure. The α/β Si_3N_4 composites with a microstructure of rod-like β-Si_3N_4 grains embedded in fine, hard α-Si_3N_4 matrix may be a promising material, with a good combination of hardness and fracture toughness [14]. Systematic quantification of the α/β-phases at different sintering times is on going [20].

Fig. 6 shows X-ray diffraction patterns of the M3-series specimens. All these samples having 8 wt% total additives were sintered at 1500 °C at different holding times; namely 0, 3 and 20 min. The 0 min set specimen is to be taken as reference. The 3 min sample triggered a significant α → β phase transformation with a consequent densification improvement (Fig. 1). This suggests that used additives have provided enough energy on the surface of Si_3N_4 particles as to react forming a glassy phase [9–11], which may in turn dissolve the alpha phase. Looking at the X-ray pattern of the 3 min sinter-hold-time specimen, specifically from 40 to 90 ($2\theta^\circ$) no intense diffraction peaks are observed. Since the chemical composition of this liquid phase was not possible to be analyzed, we assume that at this stage of the sintering process the largest amount of glassy phase might be formed (which cannot be contrasted in the XRD pattern), whereas more alpha phase is consumed to form larger and hexagonal β-Si_3N_4 grains.

Specimens of the 3M-series, having 8 wt% total additives, sintered for 3 min were fractured and analyzed by SEM. Fig. 7(a) shows a representative view of those sintered bodies disclosing the typical rod-like shape of hexagonal β-Si_3N_4 crystals. Not having a perfect orientation but being nearly regular in size and length such thick-fibrous grains grown forming the so called interlocked microstructures [1]. That random distribution might eventually enhance bulk density and mechanical properties. Thus, such interlocking microstructures have been obtained in this work by using super fast heating rates without any seeding. Fig. 7(b) is a close up view of such fractured zones. At the center of this picture an enlarged and thicker β-Si_3N_4 rod is seeing. Some other zones of this 3M-series disclosed larger rod/fibers as those seen in Fig. 8(a). If longer soaking time is allowed upon the sintering course and/or if there is a local concentration of energy in the microstructure of the ceramic material, β-Si_3N_4 crystals will further develop at the expense of their alpha counterpart.

To be noted in Fig. 8(a) is the inside-conical shape of the β-Si_3N_4 crystals. Fig. 8(b) shows the lacking part of the later; i.e., the

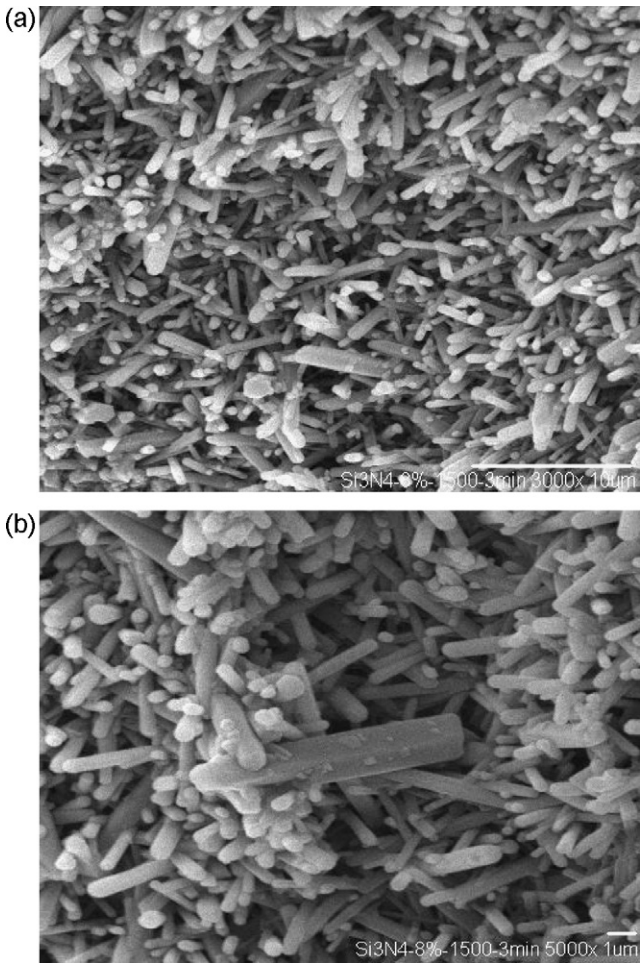

Fig. 7. (a) Fractured surface of M3-specimens (92 wt%Si_3N_4–5Y_2O_3–3Al_2O_3) densified at 1500 °C for 3 min. (b) Fractured surface of M3-specimens (92 wt%Si_3N_4–5Y_2O_3–3Al_2O_3) densified at 1500 °C for 3 min. Rod-like and hexagonal β-Si_3N_4 crystals eventually grown if sintering time is extended (look rod at center of photo).

outside conical shape counterpart, which completes the geometric assembly. It is known that in the course of α- to β-phase transformation, typically taking place around 1420 °C in pure silicon nitride Si_3N_4 ceramics there is a reduction on the crystallographic cell parameters, specifically along the *c*-axis. The *c*-spacing of α-Si_3N_4 is approximately twice that of β-phase. The longer stacking sequence is responsible for the higher hardness of α-Si_3N_4 because of the longer Burgers vector required for slip dislocation [14]. The later fact influences the mechanical properties of ideally fabricated dense Si_3N_4, apart from the resulting elongated β-grains as well as the overall grain size of these ceramics.

Fig. 9(a) shows another view of the hexagonal β-Si_3N_4 crystals presented in Fig. 8(b). Note the flat-terrace step being developed on top of one face of the largest crystal shown. Raw material required to build up such step is provided from the alpha phase through the concept of step-edge-ions [19]. To the right of the largest crystal shown in this figure it is observed a smaller one (also hexagonal) considered to be in full growth. Under the largest crystal shown in same Fig. 9(a) there is a five faces crystal, which is on its way to become hexagonal (see Fig. 9(b and c)). All these crystals are embedded into the activated α-Si_3N_4 matrix. The properties, crystallographic orientation and growing mechanism of such steps in β-Si_3N_4 needs further study.

Preliminary work focused to analyze the morphology evolution of α-Si_3N_4 powder along the SPS-treatment [20] has revealed that

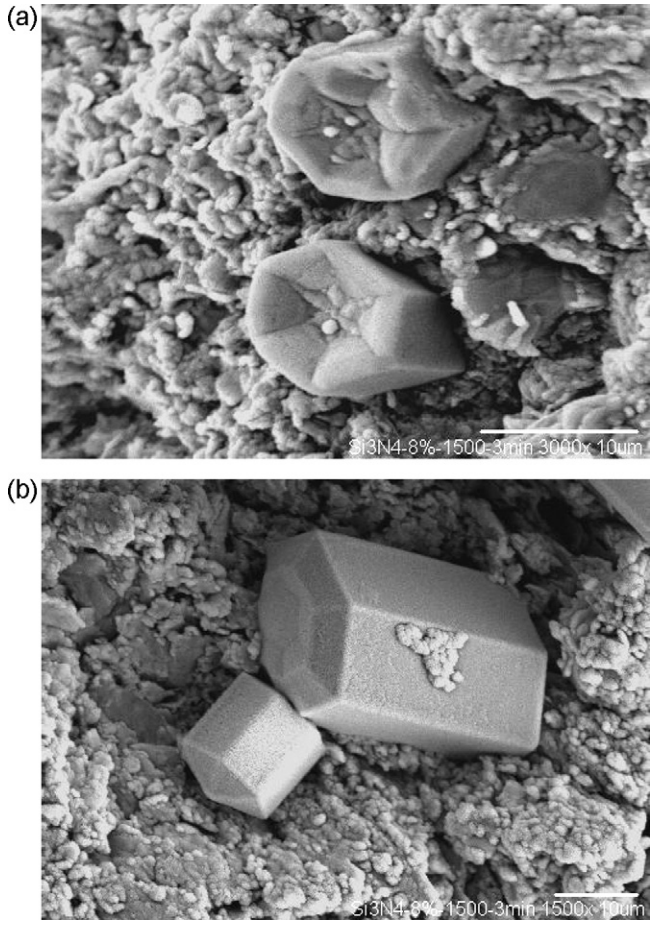

Fig. 8. (a) Fractured surface of M3-specimens (92 wt%Si_3N_4–$5Y_2O_3$–$3Al_2O_3$) densified at 1500 °C for 3 min. Rod-like and hexagonal β-Si_3N_4 crystals eventually grown if energy is concentrated on specific zones upon sintering. Note the inside-conical shape of crystals. (b) Fractured surface of M3-specimens (92 wt%Si_3N_4–$5Y_2O_3$–$3Al_2O_3$) densified at 1500 °C for 3 min. Hexagonal β-Si_3N_4 crystals eventually can grow if energy is concentrated on specific zones upon sintering. Note the outside-conical shape of crystals. When this crystal breaks apart its bottom shows the inside-conical shape.

precursor powder having soft agglomerates (Fig. 3) undergo crystalline and geometric transformations. The intermediate shapes disclosed by Si_3N_4 crystals before adopting the hexagonal shot-views as shown through Figs. 7–9, are deformed cubic (look at the particle placed immediately under hexagonal crystal in Fig. 9(a–c)) disclosing four and five fold coordinated faces. Hexagonal crystals once formed keep on growing as seen in right side of Fig. 9(a), up to the size of the largest crystal shown in same figure (see also Fig. 8(b)).

Fig. 10 represents a schematic of the geometric changes suffered by the α-Si_3N_4 particles along SPS. At the first sintering stages particles adopted a prismatic arrangement of four faces with a prismatic crown, so that on further heating another face became evident but still having short length faces. At higher temperatures, the later geometries enlarge revealing the β-Si_3N_4 rods growth. In agreement with the last draw (left to right), Fig. 9(a) demonstrates the way such rods get thicker throughout the step-edge concept [19].

Vickers hardness measurements could only be conducted on M2 and M3-series, since M1 specimens were so fragile and porous to be handled. Fig. 11 shows hardness data of M2 and M3-series plotted versus the holding time upon sintering, using the amount of additives described in Table 1. The best hardness value attained in this experiments developed a maximum of 1588 Hv and corresponded to the M3-series (1500 °C/20 min), which had the largest amount

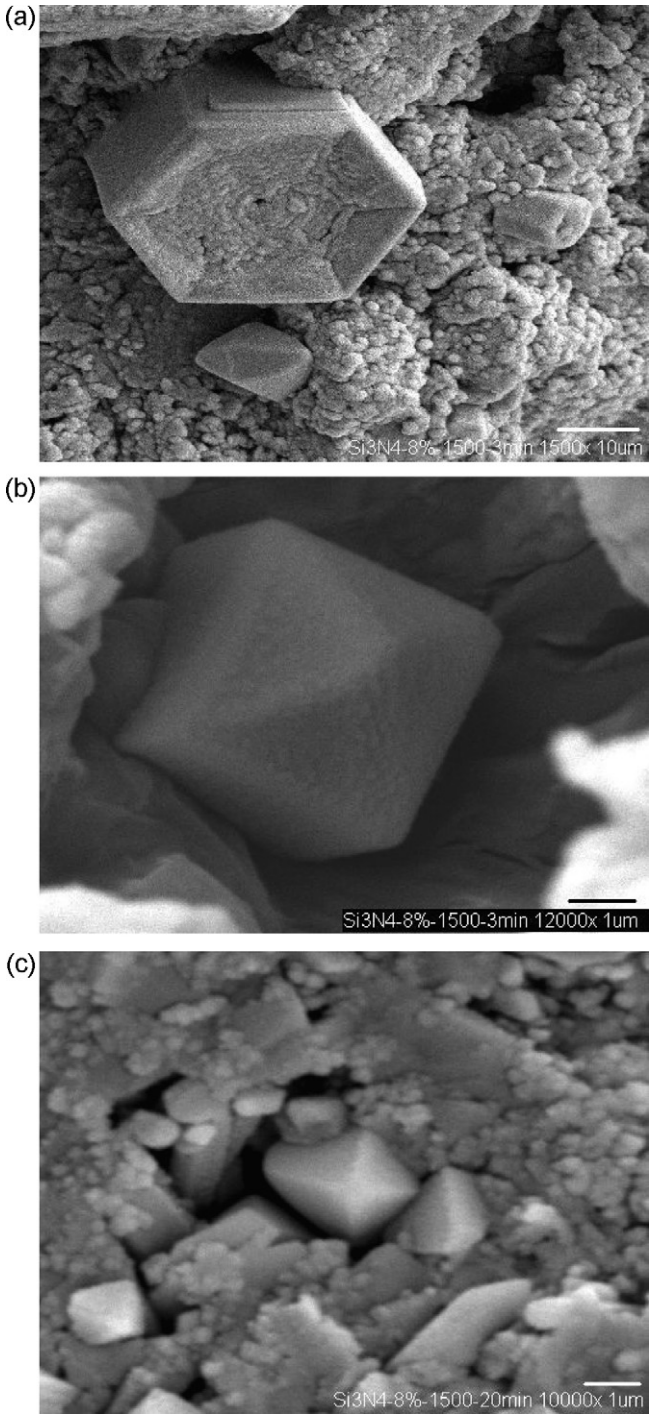

Fig. 9. (a) Fractured surface of M3-specimens (92 wt%Si_3N_4–$5Y_2O_3$–$3Al_2O_3$) densified at 1500 °C for 3 min. Hexagonal β-Si_3N_4 crystals eventually grown if energy is concentrated on specific zones upon sintering. Note the flat-floor being developed on top of the largest crystal shown. (b) and (c) Fractured surface of M3-specimens (92 wt%Si_3N_4–$5Y_2O_3$–$3Al_2O_3$) densified at 1500 °C for 3 and 20 min, respectively. (b) Cubic/pyramidal morphology of Si_3N_4 crystals on its way to adopt hexagonal forms. (c) A similar particle as in (a), seen at the center of picture showing 5-bold faces (see Fig. 10).

of additives. Smith and Hashemi [21], reported 1600 Hv for a similar material consolidated by conventional routes at sintering times longer than 1 h. SEM observations revealed that the microstructure of our specimens was not β-phase rich; i.e., our specimens still contain a given amount of α-phase. Gui-hua et al. reported the hardest α/β-Si_3N_4 composites for specimens retaining 79 wt% α-Si_3N_4,

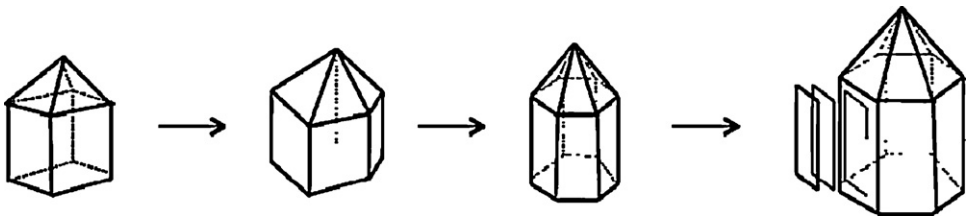

Fig. 10. Schematic representation of the geometric transformation observed in particles of doped Si_3N_4-composites, sintered by SPS at 1500 °C. As long as heating takes place a new face developed, from 4- to 6-fold faces before turning into a thick rod.

Table 2
Relative density comparative results of silicon nitride ceramics sintered with different techniques and conditions.

Powder (wt%)	Additives (wt%)				Sintering conditions				Relative	References
α or β-Si_3N_4	Al_2O_3	Y_2O_3	MgO	SiO_2	Technique	T (°C)	t (min)	P (MPa)	Density (%)	
α-92	–	3.0	5.0	–	PLS	1700	60	100[a]	97.0	[18]
α-91	–	4.0	5.0	–	PLS	1700	60	100[a]	99.0	[18]
α-91	4.0	5.0	–	–	HP	1750	120	50	99.9	[22]
α-92	–	5.0	–	3.0	PLS	1850	120	200[a]	98.4	[23]
α-92	3.0	5.0	–	–	PLS	1850	120	200[a]	99.9	[23]
α-91	3.5	5.0	–	–	GPS	1850	30	10	99.8	[24]
α-90	6.67	3.33	–	–	HP	1750	60	20	98.2	[25]
β-93	–	5.0	2.0	–	SPS	1600	10	49	98.5	[26]
α-	Yes	Yes	–	Yes	SPS	1600	–	50	–	[1]
α-	3.0	5.0	–	–	SPS	1500	Several	30	>99.0	[27]
α-94	Yes	Yes	–	–	SPS	1650	5	30	93.0	[16]
α-	–	–	Yes	Yes	SPS	1500	Several	60	100.0	[14]
α-100	–	–	–	–	SPS	1500	20	38	63.0	Tw
α-96	1.5	2.5	–	–	SPS	1500	20	38	90.3	Tw
α-92	3.0	5.0	–	–	SPS	1500	3	38	99.6	Tw
α-92	3.0	5.0	–	–	SPS	1500	20	38	99.8	Tw

Code: GPS = gas pressure sintering, PLS = pressure-less sintering, HP = hot-pressing, SPS = spark plasma sintering.
Tw = this work.
[a] Cold-pressing treatment.

comparing it with α-Sialon ceramics and argued to be harder than ordinary β-Si_3N_4 ceramics [14]. Under the sintering conditions set in this work, it is found that longer sintering times does not necessarily lead to higher hardness (see two bottom lines in Table 2) but grain growth and phase transformation throughout enlargement of β-Si_3N_4 rods.

For comparison purposes, Table 2 summarizes the relative density of Si_3N_4 specimens developed by using different techniques and experimental conditions, including SPS. It is worth saying that depending on the kind of application sought for those specimens the most convenient sintering technique is to be chosen. In spite of being fabricated in shorter sintering times and lower temperatures, having controlled microstructures and larger density, the main disadvantage found from SPS treated specimens is the final size of obtained pieces. The later being, in fact, a limitation imposed by the kind of SPS-device used. In general, SPS shows the possibility of fabricating high dense α/β-Si_3N_4 composites from 1500 °C in less than 30 min at low pressures providing the presence of sintering additives.

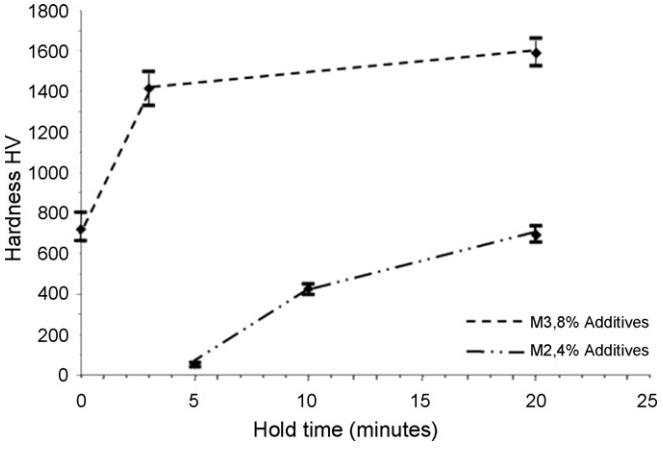

Fig. 11. Vickers hardness measurements conducted on M2 and M3-series specimens.

4. Conclusions

The spark plasma sintering SPS technique has been used to densify pure α-Si_3N_4 commercial powder, having Y_2O_3 and Al_2O_3 additions; from 0, 2.5 and 5.0 wt% to 0, 1.5 and 3 wt%, respectively. In all studied cases, the relative density developed by increasing the amount of additives. It is confirmed that if no additives were used into the α-Si_3N_4 powder matrix, there will be no densification or phase transformation. SPS has shown the possibility of fabricating high dense α/β-Si_3N_4 composites from 1500 °C in less than 30 min at low pressures providing the presence of sintering additives. The maximum relative density developed on studied specimens ranged from 99.4 to 99.8% and could only be attained once the β-phase nucleated from the α-silicon nitride matrix. The best hardness value attained in this experiments developed a maximum of 1588Hv and corresponded to the M3-series (1500 °C/20 min), which had the largest amount of additives.

SEM and XRD analyses revealed that obtained Si_3N_4 composites combine both α- and β-phases. The later phase becomes evident trough the typical β-Si_3N_4 rod-like geometry, which is known to form throughout the presence of a liquid face. The α/β Si_3N_4 composites with a microstructure of rod-like β-Si_3N_4 grains embedded in fine, hard α-Si_3N_4 matrix may be a promising material, with a sufficient hardness, as compared to counterpart-specimens reported in literature. Not having a perfect orientation

but being nearly regular in size and length such thick-fibrous grains grown forming the so called interlocked microstructures. That random distribution might eventually enhance bulk density and mechanical properties. Interlocking microstructures have been obtained in this work by using super fast heating rates without any seeding.

The morphology evolution of Si_3N_4 particles as occurred upon SPS-sintering has been analyzed. SEM analysis revealed hexagonal β-Si_3N_4 crystals with a flat-terrace step being developed on top of one face. Raw material required to build up such step is provided from the alpha phase through the concept of step-edge-ions [19]. This preliminary work focused to analyze the morphology evolution of α-Si_3N_4 powder along the SPS-treatment has revealed that precursor powder having soft agglomerates undergo crystalline and geometric transformations. The intermediate shapes disclosed by Si_3N_4 crystals before adopting the hexagonal shot-views are deformed cubic arrangements, disclosing four and five fold coordinated faces with a prismatic crown. Hexagonal crystals once formed keep on growing. Under the sintering conditions set in this work, it is found that longer sintering times does not necessarily lead to higher hardness (see two bottom lines in Table 2) but grain growth and phase transformation throughout enlargement of β-Si_3N_4 rods.

A schematic representation of the geometric changes suffered by the α-Si_3N_4 particles along SPS is given in this work.

Acknowledgements

This work is part of a doctoral thesis (LCC) partially supported through the project No. PIFUTP08-110, sponsored by the Instituto de Ciencia y Tecnología del Distrito Federal ICyTDF, Mexico. Authors thank to Red Nacional de Nanotecnología del Instituto Politécnico Nacional for the facilities (SPS) used in this research. Authors also acknowledge to CONACyT-SNI, Mexico.

References

[1] Z. Shen, Z. Zhao, H. Peng, M. Nygren, Lett. Nat. 417 (2002) 266–269.
[2] C.C. Liu, Ceram. Int. 29 (2003) 841–846.
[3] V.V. Vikulin, Adv. Sci. Technol. 45 (2006) 1751–1758.
[4] O. Chimal-Valencia, M.S. Corral-García, H. Kume, Y. Nishikawa, M. Iwasa, S.D. de la Torre, Key Eng. Mater. Trans. Technol. Pub. 317–318 (2006) 389–392.
[5] W.E. Lee, W.M. Rainforth (Eds.), Ceramic Microstructure, Property Control by Processing, Chapman & Hall, Shefield, UK, 1994, 388–390 (chapter 7).
[6] P. Bhandhubanyong, T. Akhadejdamrong, J. Mater. Process. Technol. 63 (1997) 277–280.
[7] A. Vuckovic, B. Matovic, S. Buskovic, Mater. Sci. Forum 494 (2005) 429–434.
[8] M. Tokita, Mechanism of spark plasma sintering, in: K. Kosuge, H. Nagai (Eds.), Proceedings of the 2000 Powder Metallurgy World Congress, Kyoto, Japan. Nov. 2000. Ed. Japanese Soc. of Powder & Powder Met. Kyoto Japan, 2001, pp. 729–732.
[9] R.G. Duan, G. Roebben, J. Vleugels, O. Van der Biest, J. Eur. Ceram. Soc. 22 (2002) 1897.
[10] G. Roebben, R.G. Duan, D. Sciti, O. Van der Biest, J. Eur. Ceram. Soc. 22 (2002) 2501.
[11] H.J. Kleebe, M.K. Cinibulk, R.M. Cannon, M. Ruler, J. Am. Ceram. Soc. 76 (1993) 1969.
[12] M. Mitomo, Y. Tajima, J. Ceram. Soc. Jpn. 99 (10) (1991) 1014.
[13] F. Chen, Q. Shen, F. Yan, L. Zhang, Mater. Chem. Phys. 107 (2008) 67–71.
[14] P. Gui-hua, L. Xiang-guo, L. Min, L. Zhen-hua, L. Qian, Li Wen-lan, Scr. Mater. 61 (2009) 347–350.
[15] J. Wan, R.G. Duan, A.K. Mukherjee, Scr. Mater. 53 (2005) 663–667.
[16] Y. Li, L.R. Xia, L.J. Xing Z., Mater. Sci. Eng. A 483–484 (2008) 207–210.
[17] M. Kitayama, K. Hirao, M. Toriyama, S. Kanazaki, Acta Mater. 46 (1998) 6541–6550.
[18] G. Ling, H. Yang, Mater. Chem. Phys. 90 (2005) 31–34.
[19] V.E. Henrich, P.A. Cox (Eds.), The Surface Science of Metal Oxides, Cambridge University Press, 1994, p. 64.
[20] L. Ceja-Cardenas, Doctor Thesis. Universidad Michoacana de San Nicolás de Hidalgo, Mexico, 2011.
[21] W.F. Smith, J. Hashemi (Eds.), Fundamentos de la ciencia e ingeniería de materiales, 4th ed., Mc Graw Hill, Mexico, 2007.
[22] M. Belmonte, A. de Pablos, M.I. Osendi, P. Miranzo, Mater. Sci. Eng. A 475 (2008) 185–189.
[23] T. Wasanapiarnpong, S. Wada, M. Imai, T. Yano, J. Eur. Ceram. Soc. 26 (2006) 3467–3475.
[24] C.V. Rocha, C.A. Costa, Mater. Res. 9 (2006) 143–146.
[25] L. Bai, X.Y. Zhao, C.C. Ge, Mater. Sci. Forum 546–549 (2007) 2179–2182.
[26] T. Nishimura, M. Mitomo, H. Hirotsuru, M. Kawahara, J. Mater. Sci. Lett. 14 (1995) 1046–1047.
[27] M. Sugunama, Y. Kitagawa, J. Am. Ceram. Soc. 86 (3) (2003) 387–394.